Article

Cell Reports

Targeting Macrophages Sensitizes Chronic Lymphocytic Leukemia to Apoptosis and Inhibits Disease Progression

Graphical Abstract

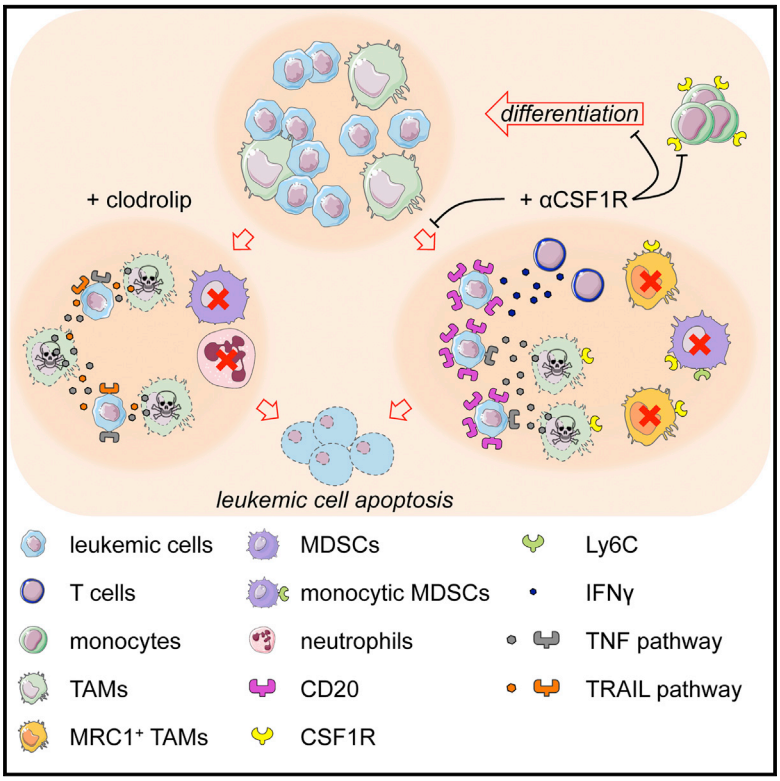

Highlights

- The macrophage transcriptome is modulated by leukemic cells
- Macrophage depletion limits survival of leukemic cells in vivo
- Macrophage killing restores apoptosis sensitivity of leukemic cells
- Macrophage targeting can be therapeutically exploited in CLL

Authors

Giovanni Galletti, Cristina Scielzo, Federica Barbaglio, ..., Michele De Palma, Federico Caligaris-Cappio, Maria Teresa Sabrina Bertilaccio

Correspondence

federico.caligaris@airc.it (F.C.-C.), bertilaccio.sabrina@hsr.it (M.T.S.B.)

In Brief

CLL is the prototype of chronic B cell tumors, and its development and progression depend on a complex network of cells including macrophages. Galletti et al. describe a set of molecular interactions supporting the in vivo dependence of leukemic cells on monocytes/macrophages and suggest therapeutic strategies based on macrophage targeting.

Accession Numbers

GSE57787
GSE57785

Galletti et al., 2016, Cell Reports *14*, 1–13
February 23, 2016
http://dx.doi.org/10.1016/j.celrep.2016.01.042

CellPress

Please cite this article in press as: Galletti et al., Targeting Macrophages Sensitizes Chronic Lymphocytic Leukemia to Apoptosis and Inhibits Disease Progression, Cell Reports (2016), http://dx.doi.org/10.1016/j.celrep.2016.01.042

Cell Reports
Article

Targeting Macrophages Sensitizes Chronic Lymphocytic Leukemia to Apoptosis and Inhibits Disease Progression

Giovanni Galletti,[1,2] Cristina Scielzo,[1,2] Federica Barbaglio,[1] Tania Véliz Rodriguez,[1] Michela Riba,[3] Dejan Lazarevic,[3] Davide Cittaro,[3] Giorgia Simonetti,[4] Pamela Ranghetti,[1] Lydia Scarfò,[5,6] Maurilio Ponzoni,[6,7] Martina Rocchi,[6,7] Angelo Corti,[8] Achille Anselmo,[9] Nico van Rooijen,[10] Christian Klein,[11] Carola H. Ries,[12] Paolo Ghia,[2,5,6] Michele De Palma,[13,14] Federico Caligaris-Cappio,[1,2,6,15,*] and Maria Teresa Sabrina Bertilaccio[1,2,15,*]

[1]Unit of Lymphoid Malignancies, Division of Experimental Oncology, IRCCS San Raffaele Scientific Institute, 20132 Milan, Italy
[2]Vita-Salute San Raffaele University, 20132 Milan, Italy
[3]Center for Translational Genomics and Bioinformatics, IRCCS San Raffaele Scientific Institute, 20132 Milan, Italy
[4]Department of Experimental, Diagnostic and Specialty Medicine, Institute of Hematology "L. e A. Seràgnoli," Università di Bologna, 40138 Bologna, Italy
[5]Unit of B Cell Neoplasia, Division of Experimental Oncology, IRCCS San Raffaele Scientific Institute, 20132 Milan, Italy
[6]Unit of Lymphoid Malignancies, Department of Onco-Hematology, IRCCS San Raffaele Hospital, Milan, Italy
[7]Pathology Unit, IRCCS San Raffaele Scientific Institute, 20132 Milan, Italy
[8]Tumor Biology and Vascular Targeting Unit, Division of Experimental Oncology, IRCCS San Raffaele Scientific Institute, 20132 Milan, Italy
[9]Humanitas Clinical and Research Center, 20089 Rozzano, Milan, Italy
[10]Department of Molecular Cell Biology, Vrije University Medical Center, 1081 BT Amsterdam, the Netherlands
[11]Roche Pharma Research and Early Development, Oncology Discovery, Roche Innovation Center Zurich, 8952 Zurich, Switzerland
[12]Roche Pharmaceutical Research and Early Development, Roche Innovation Center Penzberg, Oncology Discovery, 82377 Penzberg, Germany
[13]The Swiss Institute for Experimental Cancer Research (ISREC), School of Life Sciences, École Polytechnique Fédérale de Lausanne (EPFL), 1015 Lausanne, Switzerland
[14]Division of Regenerative Medicine, Stem Cells and Gene Therapy, IRCCS San Raffaele Scientific Institute, 20132 Milan, Italy
[15]Co-senior author
*Correspondence: federico.caligaris@airc.it (F.C.-C.), bertilaccio.sabrina@hsr.it (M.T.S.B.)
http://dx.doi.org/10.1016/j.celrep.2016.01.042

SUMMARY

The role of monocytes/macrophages in the development and progression of chronic lymphocytic leukemia (CLL) is poorly understood. Transcriptomic analyses show that monocytes/macrophages and leukemic cells cross talk during CLL progression. Macrophage depletion impairs CLL engraftment, drastically reduces leukemic growth, and favorably impacts mouse survival. Targeting of macrophages by either CSF1R signaling blockade or clodrolip-mediated cell killing has marked inhibitory effects on established leukemia also. Macrophage killing induces leukemic cell death mainly via the TNF pathway and reprograms the tumor microenvironment toward an antitumoral phenotype. CSF1R inhibition reduces leukemic cell load, especially in the bone marrow, and increases circulating CD20$^+$ leukemic cells. Accordingly, co-targeting TAMs and CD20-expressing leukemic cells provides a survival benefit in the mice. These results establish the important role of macrophages in CLL and suggest therapeutic strategies based on interfering with leukemia-macrophage interactions.

INTRODUCTION

The interactive co-evolution of cancer and normal bystander cells optimizes the clonal expansion of chronic lymphoid malignancies of B cell type within specific microenvironments. Chronic lymphocytic leukemia (CLL) is the most frequent and paradigmatic chronic B cell malignancy, characterized by the growth of mature CD5$^+$ monoclonal B lymphocytes in immune-protected and protumorigenic habitats that include stromal, T, and endothelial cells (Caligaris-Cappio et al., 2014; Caligaris-Cappio and Ghia, 2008; Zenz et al., 2010). CLL cells accumulating in peripheral lymphoid organs, bone marrow (BM), and circulating in peripheral blood (PB) are the progeny of cells that proliferate in specific tissue microenvironmental niches, termed pseudofollicles (Caligaris-Cappio et al., 2014).

CLL cell cross talk with the microenvironment is largely dependent upon a functional leukemic B cell receptor (BCR). Signaling through the BCR modulates CLL cell proliferation, survival, and cytoskeletal activity and can be targeted by inhibitors that, by interfering with different BCR-associated kinases such as Bruton tyrosine kinase (BTK), also influence the interaction between CLL cells and the microenvironment (Burger and Gribben, 2014; Byrd et al., 2013). For example, the BTK inhibitor ibrutinib blocks the protective functions of stromal cells (Herman et al., 2011), which deploy signals that favor the survival of CLL cells (Lutzny et al., 2013).

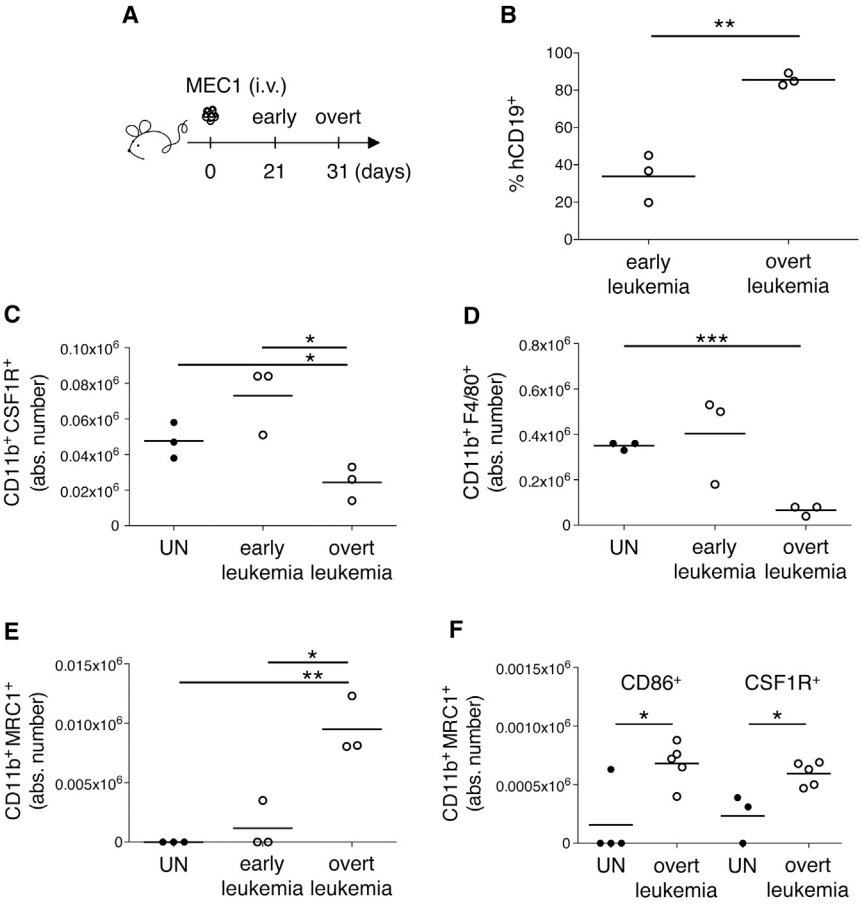

Figure 1. BM Microenvironment of Xeno-transplanted Mice: Monocyte and Macrophage Populations

(A–F) Rag2$^{-/-}\gamma c^{-/-}$ mice, uninjected (UN, black circles) or injected i.v. with MEC1 (white circles) cells (day 0), were killed at early (n = 3) and late (n = 3) stage of leukemia and analyzed by flow cytometry (A). The mean value of the relative contribution of hCD19$^+$ cells in BM is shown in (B). The mean value of the absolute number of CD11b$^+$ CSF1R$^+$ cells gated on CD45$^+$ in BM is shown in (C). The mean value of the absolute number of CD11b$^+$ F4/80$^+$ cells gated on CD45$^+$ in BM is shown in (D). The mean value of the absolute number of CD11b$^+$ MRC1$^+$ cells to the whole macrophage pool (CD11b$^+$ F4/80$^+$) gated on CD45$^+$ in BM is shown in (E). Data are from one representative experiment out of three. Statistical analysis: *p < 0.05, **p < 0.01, and ***p < 0.001, Student's t test.

(F) The mean value of the absolute number of CD86$^+$ MRC1$^+$ and CSF1R$^+$ MRC1$^+$ cells to the whole CD45$^+$ CD11b$^+$ pool in BM is shown. Statistical analysis: *p < 0.05, Student's t test.

See also Figure S1.

A role for monocyte/macrophage cells in CLL has been suggested by a number of in vitro and correlative studies. The survival of leukemic cells is supported in vitro by nurse-like cells (NLCs) that are induced upon coculturing PB or spleen monocytes with CLL cells (Tsukada et al., 2002). NLCs share lineage and functions with lymphoma-associated macrophages described in other B cell tumors and have been identified as CLL-specific tumor-associated macrophages (TAMs) (Filip et al., 2013). The gene expression profile (GEP) of CLL cells exposed in vitro to NLCs (Burger et al., 2009) is strikingly similar to that of CLL cells isolated from lymph nodes (Herishanu et al., 2011). Moreover, the absence of macrophage migration inhibitory factor (MIF) was shown to delay the development of leukemia in the *Eμ-TCL1* transgenic mouse model of CLL (Bichi et al., 2002; Reinart et al., 2013).

Prompted by these observations, we sought to investigate the mechanisms whereby TAMs regulate leukemic cell growth in vivo by employing different CLL transplantation mouse models and TAM depletion strategies. In particular, we employed a cell-killing approach based on the macrophage uptake of clodronate (Acquati et al., 2011; van Rooijen and Hendrikx, 2010) and an anti-colony-stimulating factor-1 receptor (CSF1R) monoclonal antibody (mAb). The therapeutic anti-CSF1R mAb emactuzumab (RG7155) inhibits macrophage differentiation from monocyte precursors and is emerging as clinical tool to target macrophages (Ries et al., 2014; Ruffell and Coussens, 2015). Our findings demonstrate that TAMs critically support the survival and proliferation of CLL cells in vivo, therefore unveiling therapeutic strategies based upon manipulating TAM/CLL-cell interactions.

RESULTS

Characterization of BM Monocytes and Macrophages in CLL Xeno-transplanted Mice

We asked whether monocytes/macrophages influence CLL growth in the BM. Eight-week-old Rag2$^{-/-}\gamma_c^{-/-}$ mice were injected intravenously (i.v.; day 0) with MEC1 cells (a CLL cell line) (Bertilaccio et al., 2010) and killed either in the early (day 21) or overt (day 31) phase of leukemia growth (Figure 1A), when the percentage of human CD19$^+$ leukemic cells in the BM was 33.83 ± 15.03 and 86 ± 9.13, respectively (Figure 1B). We found lower numbers of CD11b$^+$CSF1R$^+$ monocytes and CD11b$^+$F4/80$^+$ macrophages in the BM of frank leukemic Rag2$^{-/-}\gamma_c^{-/-}$ mice when compared to early leukemic mice (Figures 1C and 1D). While the total F4/80$^+$ macrophage population decreased, the abundance of CD11b$^+$ cells coexpressing the macrophage mannose receptor (MRC1/CD206), CSF1R, and CD86 increased along with leukemia progression (Figures 1E and 1F), a feature also associated with progression of solid tumors (De Palma and Lewis, 2013; Noy and Pollard, 2014).

To specifically characterize the molecular profile of CLL-associated monocytes/macrophages (Figures 1C and 1D), a

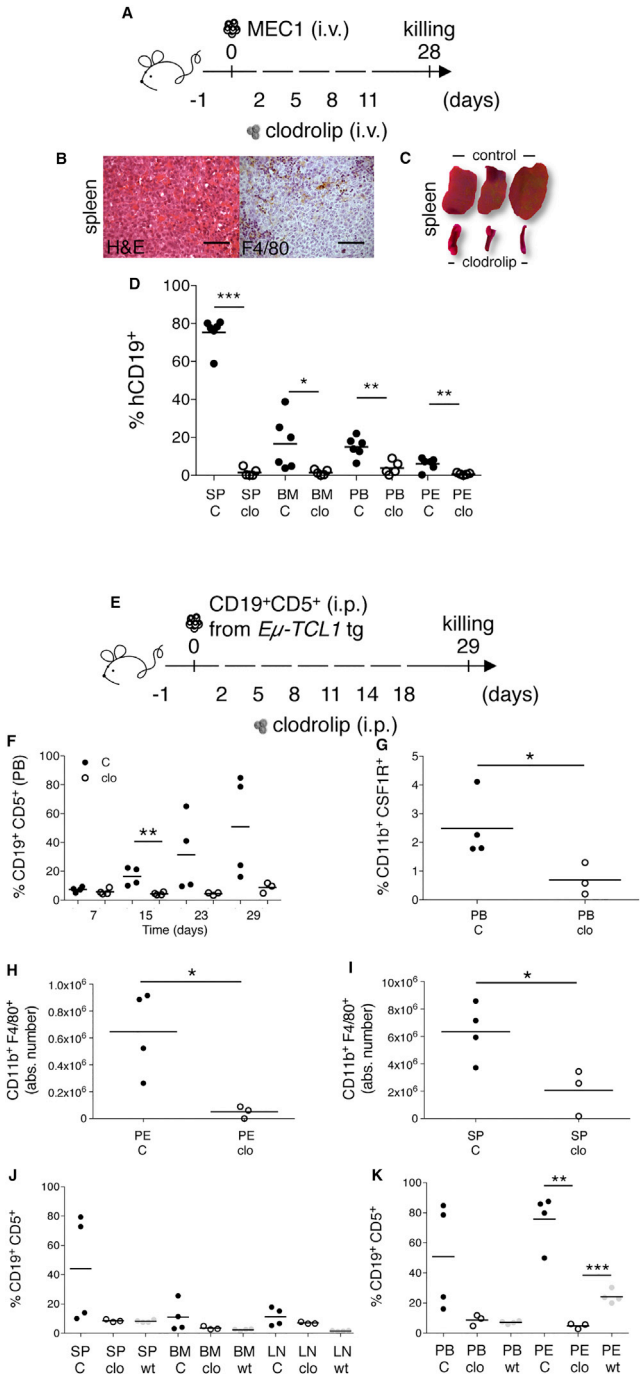

Figure 2. Effect of Clodrolip-Mediated Macrophage Depletion in CLL Transplantation Systems

(A–D) Rag2$^{-/-}\gamma c^{-/-}$ mice, injected i.v. with MEC1 cells (day 0) and macrophage-depleted by i.v. injection of PBS liposomes (200 μl, black circles, C) or clodrolip (200 μl, white circles, clo) every 3 days starting at day −1 were sacrificed at day 28 (A). Histology of spleen is shown (one representative mouse): H&E staining and immunohistochemistry stain for murine F4/80; scale bars, 100 μm (B). Spleens from control and clodrolip-treated mice were collected and analyzed macroscopically; for control mice, half the spleen is shown (C). The mean value of the relative contribution of hCD19$^+$ cells in SP, BM, PB, and PE is shown in graph (D). Data are from two independent experiments (n = 6/group). Statistical analysis: *p < 0.05, **p < 0.01, and ***p < 0.001, Student's t test.

(E–K) C57BL/6 mice transplanted i.p. with leukemic B cells from *Eμ-TCL1* transgenic mouse, pretreated i.p. (day −1) with 200 μl PBS liposomes (n = 4, black circles) or with clodrolip (n = 4, white circles), were analyzed by flow cytometry (E). The mean value of the relative contribution of CD19$^+$ CD5$^+$ cells to the whole B cell pool in PB over time is shown (F). The mean value of the relative contribution of CD11b$^+$ CSF1R$^+$ cells gated on CD45$^+$ in PB is shown (G). The mean value of the absolute number of CD11b$^+$ F4/80$^+$ cells gated on CD45$^+$ in PE and SP is shown in (H) and (I), respectively. The mean value of the relative contribution of CD19$^+$ CD5$^+$ cells to the whole B cell pool in SP, BM, lymph node (LN) (J), and PB and PE (K) at day 29 is shown. Data are from one representative experiment of two. Statistical analysis: *p < 0.05, **p < 0.01, and ***p < 0.001, Student's t test.

whole-genome transcriptional profile analysis was performed by Illumina hybridization system on monocytes/macrophages isolated from the BM of Rag2$^{-/-}\gamma c^{-/-}$ xeno-transplanted mice, sacrificed at day 21 (early leukemia). A complex network of gene regulation involving the modulation of 164 transcripts (84 up- and 80 downregulated; 1.6% of total transcripts; adjusted p value < 0.05) distinguished monocytes/macrophages of mice with leukemia compared to age-matched, uninjected mice (Table S1). Differentially expressed genes were organized into five putative functional categories including inflammation and intracellular/extracellular function, shown in Figures S1A–S1E. In parallel, we also analyzed the transcriptional changes occurring in leukemic MEC1 cells purified from the same mice. Particularly relevant was the differential expression of genes supporting the existence of monocyte/macrophage-leukemic cell cross talk, including *IL10*, *RNASET2*, and *CCL2* (a potent monocyte chemoattractant; Noy and Pollard, 2014), besides genes involved in CLL progression, like *NOTCH1*, *BIRC3*, and *PTEN* (Figure S1F). Due to its role in B cell adhesion, antigen presentation, and activation (Batista and Harwood, 2009), we validated ICAM1 upregulation at the protein level, both in mouse macrophages from spleen (SP), BM, or peritoneal exudate (PE) (Figure S1G) and human classical monocytes of CLL patients (Figure S2A). Xeno-transplantation studies using an anti-mouse ICAM1 blocking mAb, administered every 3/4 days from day −1 (Figure S2B), demonstrated that its inhibition increased the number of leukemic cells in the PB, SP, and PE, but not in the BM (Figure S2C), thus suggesting a functional relevance of ICAM1 upregulation in different tissues. We also confirmed by qPCR the differential expression of a panel of selected genes in both murine monocytes/macrophages (Figure S2D) and human MEC1 cells (Figure S2E).

Taken together, these findings indicate that CLL cells profoundly sculpt the BM microenvironment and modulate the expression of multiple gene transcripts involved in CLL cell-monocyte/macrophage interaction.

Macrophage Depletion Impairs CLL Grafting in Mice

The aforementioned analyses led us to investigate whether CLL engraftment and progression in mice might be affected by the absence of monocytes/macrophages. To address this question, we depleted macrophages in MEC1-grafted Rag2$^{-/-}\gamma c^{-/-}$ mice by i.v. administration of clodronate liposomes (clodrolip) every 3 days from day −1 (Figure 2A), as described previously

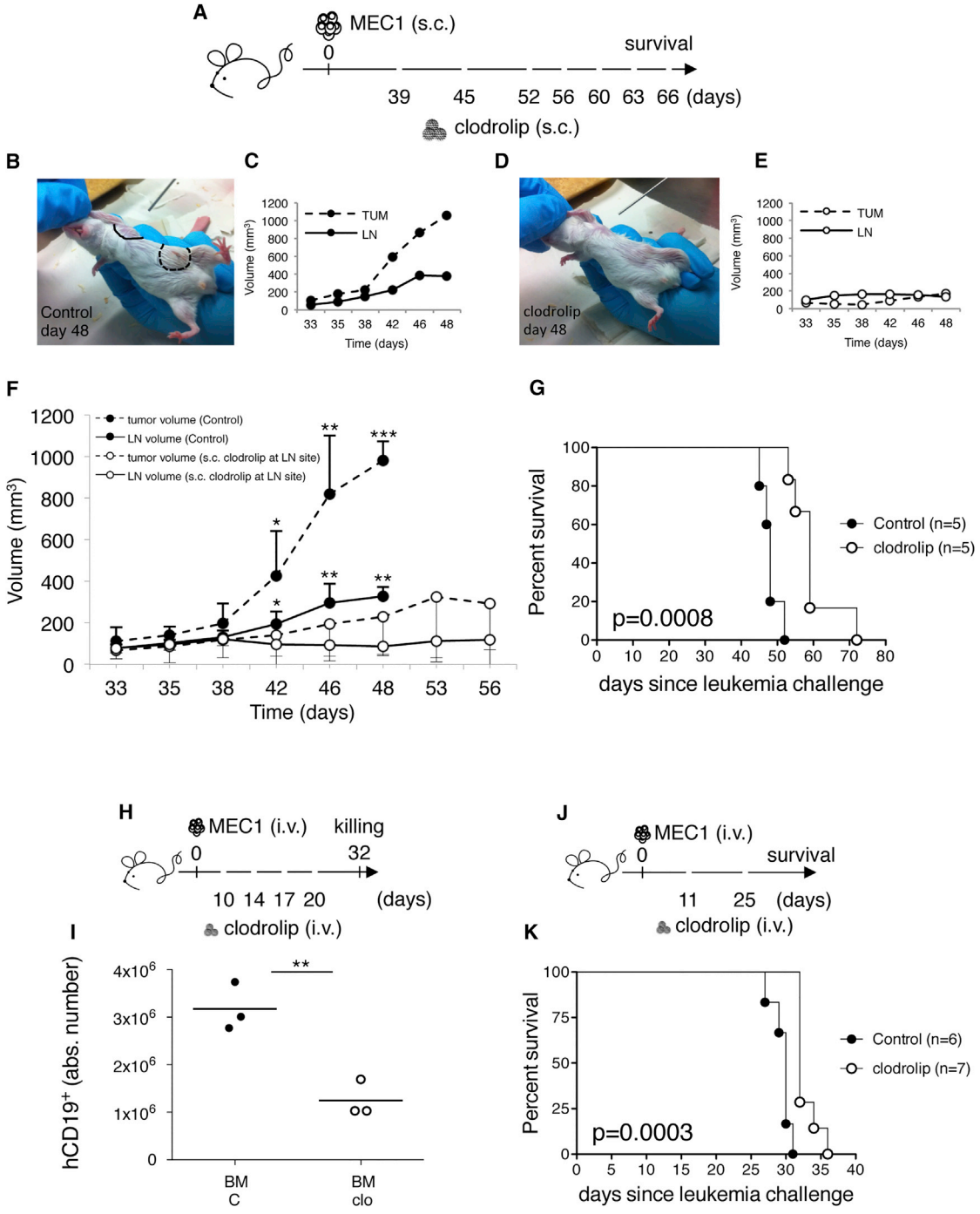

Figure 3. Monocyte/Macrophage Killing Approach in CLL Xenograft Systems at the Preclinical Level

(A–G) Rag2$^{-/-}\gamma c^{-/-}$ mice transplanted s.c. with MEC1 cells were treated s.c. at the LN site (days +39, +45, +52, +56, +60, +63, and +66) with 50 μl of PBS liposomes (n = 5, black circles) or clodrolip (n = 5, white circles) (A). A representative mouse (day 48) with its tumor (dashed line) and LN (continuous line) growth curves are shown for PBS liposomes (B and C) and clodrolip (D and E). Tumor and LN volumes (mean ± SD) are shown (F). Statistical analysis was performed using the Student's t test (*$p < 0.05$, **$p < 0.01$, and ***$p < 0.001$; measurements were stopped when 60% of mice were still surviving). These two groups of mice were monitored for survival (G). Kaplan-Meier survival curve is shown, statistical analyses was performed using the log-rank test (***$p < 0.001$). Data are from one representative experiment of two.

(H and I) i.v. MEC1 challenged (day 0) Rag2$^{-/-}\gamma c^{-/-}$ mice were treated i.v. (days +10, +14, +17, and +20) with 60 μl PBS liposomes (n = 3, black circles) or clodrolip (n = 3, white circles) and killed at day 32 (H). The mean value of the absolute number of hCD19^{+} cells in the BM is shown in graph (I). Statistically significant differences were calculated using the Student's t test (**$p < 0.01$).

(legend continued on next page)

(Sunderkötter et al., 2004). Mice were sacrificed at late stage of the disease, 17 days after the last clodrolip injection, when untreated mice developed signs of overt leukemia (e.g., weight loss). Clodrolip-mediated macrophage depletion (Figure 2B) was associated with a significant reduction of leukemic cell burden in the SP, BM, PB, and PE (Figures 2C and 2D).

To extend these findings to an immunocompetent mouse model, we transplanted leukemic cells from the spleen of *Eμ-TCL1* transgenic mice intraperitoneally (i.p.) into syngeneic immunocompetent recipients (Figure 2E), as described previously (Zanesi et al., 2006). A progressive expansion of the leukemic clone was detected in the PB of the transplanted mice after 3–4 weeks (Figure 2F). When the mice were macrophage-depleted by i.p. clodrolip injection, starting at day −1 (Figure 2E), a significantly lower number of leukemic B cells was observed in the PB over time (Figure 2F). Upon necropsy (day 29, 11 days after the last clodrolip injection), comparative analyses of clodrolip-treated and untreated mice showed that the depletion of monocytes (Figure 2G) and macrophages (Figures 2H and 2I) was associated with a reduction of the leukemic clone in lymphoid tissues (Figure 2J), PB, and especially PE (Figure 2K).

These findings suggest that monocytes/macrophages support the growth of CLL cells in mice.

Induced Monocyte/Macrophage Death Improves the Survival of Leukemic Mice

We then asked whether interfering with leukemic cell-macrophage interactions might translate into a survival benefit in CLL models. In a first set of experiments, clodrolip was administered to MEC1-injected Rag2$^{-/-}\gamma_c^{-/-}$ mice with advanced disease. Rag2$^{-/-}\gamma_c^{-/-}$ mice transplanted with subcutaneous tumors carrying visible leukemic lymph nodes (LN) were repeatedly injected subcutaneously (s.c.) with clodrolip, in proximity to the LN (Figure 3A). Compared to untreated mice (Figures 3B and 3C), clodrolip greatly reduced the LN size already after the second clodrolip administration (Figures 3D and 3E). Clodrolip treatment inhibited LN and primary tumor growth (Figure 3F) and extended mouse survival (Figure 3G, p = 0.0008; Figures S3A–S3G). Furthermore, when clodrolip was administered i.v. (four injections every 3 days) to systemically xeno-transplanted mice starting at day 10 after leukemic challenge (Figure 3H), it induced a significant reduction of hCD19$^+$ leukemic cells, especially in the BM (Figure 3I). Of note, two systemic administrations of clodrolip (Figure S3H) were sufficient to deplete macrophages (Figures S3I and S3J), reduce the leukemic expansion (Figures S3K and S3L), and significantly extend the survival of xeno-transplanted mice (Figures 3J and 3K).

To further test the anti-leukemic activity of clodrolip, we transplanted i.p. leukemic cells obtained from the spleen of an *Eμ-TCL1* transgenic mouse in syngeneic immunocompetent recipients. Starting at day 16 post-transplantation, the mice were injected i.p. with clodrolip every 4 days with suboptimal (non-exhaustively depleting; 50 μl/mouse) doses of clodrolip and sacrificed at day 28 (Figure S3M). As shown in Figures S3N and S3O, CD11b$^+$F4/80$^+$ macrophages were reduced in the SP and PE. We observed a significantly lower number of leukemic B cells in the PB over time (Figure S3P). A significantly lower frequency of leukemic B cells was observed in the SP, PB, and PE after four clodrolip doses (Figures S3Q and S3R), along with a significant increase of CD19$^+$CD5$^+$AnnV$^+$ early apoptotic cells in the PE, the site of leukemic cell and clodrolip injection (Figure S3S).

In conclusion, clodrolip-mediated macrophage killing is associated with a drastic reduction of CLL growth in two mouse models of the disease.

Targeting Monocytes/Macrophages by CSF1R Inhibition Can Be Exploited as a Therapeutic Strategy in CLL

To evaluate the therapeutic potential of macrophage targeting, we investigated the anti-leukemic effects of a monoclonal antibody that inhibits CSF1R signaling and prevents macrophage differentiation from monocyte precursors (Ries et al., 2014).

Rag2$^{-/-}\gamma_c^{-/-}$ mice transplanted i.v. with MEC1 cells were injected i.v. with the anti-mouse CSF1R mAb 2G2 (30 mg/kg, days +11 and +25) and sacrificed at day 27, 48 hr after the last mAb injection (Figure 4A). Macrophage depletion (Figures 4B and 4C) significantly reduced the number of leukemic B cells in the BM (Figure 4D) and induced the appearance of CD19$^+$ AnnV$^-$PI$^+$ necrotic leukemic cells in the SP (Figure 4E). To confirm that CSF1R blockade reduces disease severity in the SP, we performed a time course experiment, where mice were sacrificed 48 hr and 96 hr after the last mAb injection, at days 27 and 29, respectively (Figure 4F). CSF1R blockade was able to stabilize the disease and induce increasing necrosis of the splenic leukemic cells over time (Figure 4G). This anti-leukemic effect was associated with a remarkable and selective depletion of CSF1R$^+$ MRC1$^+$ M2-like TAMs (Figures 4H and 4I).

As already shown in solid tumors (Ries et al., 2014), CSF1R blockade, together with monocyte depletion (Figures S4A and S4B), induced a relative increase in the PB of SSC^{high} neutrophil granulocytes (Figure S4C) and Gr1$^+$ myeloid cells (Figure S4D) encompassing both monocytic (Ly6C$^+$) and granulocytic (Ly6G$^+$) subsets (Figures S4E and S4F). Of note, this effect was not observed with clodrolip (Figures S4G–S4K). In the BM, CSF1R blockade decreased monocytes, identified as either CD11b$^+$CSF1R$^+$ (Figure S4L) or Ly6C$^+$ (Figures S4M and S4N). In the *Eμ-TCL1* tg transplantation model (Figure S4O), we observed a pronounced increase of CD8$^+$ effector T cells in the PB (Figure S4P), BM (Figure S4Q), and SP (Figures S4R and S4S), accompanied by a marked increase of apoptotic leukemic cells (Figure S4T) and a decrease of splenic CD4$^+$CD25$^+$ T cells (Figure S4U). Conversely, clodrolip did not impact T cells (Figures S4V–S4X).

Two administrations of the anti-CSF1R mAb (Figure 5A) induced significant lymphocytosis (Figure 5B), a treatment-related compartment shift from infiltrated tissues into PB,

(J and K) i.v. MEC1 challenged (day 0) Rag2$^{-/-}\gamma c^{-/-}$ mice were treated i.v. (days +11 and +25) with 60 μl PBS liposomes (n = 6, black circles) or clodrolip (n = 7, white circles) and monitored for survival (J). The Kaplan-Meier survival curve is shown (K), and statistical analysis was performed using the log-rank test (***p < 0.001).

See also Figure S3.

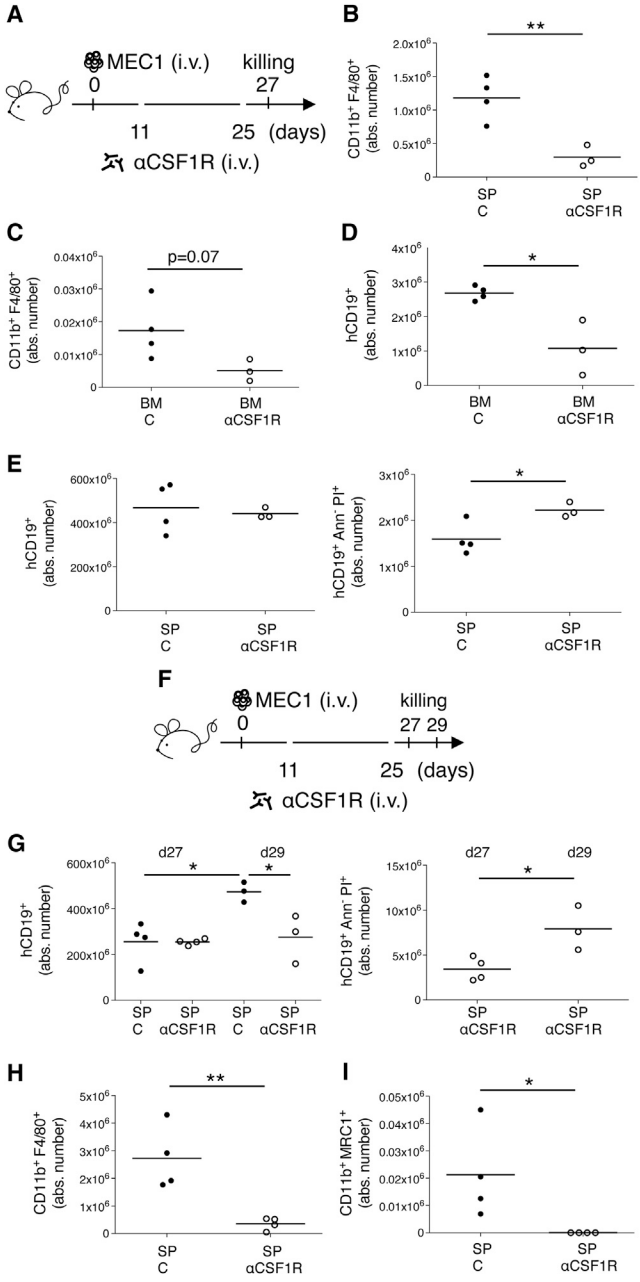

Figure 4. Anti-leukemic Effect of Anti-CSF1R mAb in the CLL Xeno-transplantation System

(A–E) i.v. MEC1 challenged (day 0) Rag2$^{-/-}\gamma c^{-/-}$ mice were treated i.v. (days +11 and +25) with 30 mg/kg anti-CSF1R mAb (n = 3, white circles) or left untreated (n = 4, black circles) and killed at day 27 (A). The mean value of the absolute number of CD11b$^+$ F4/80$^+$ cells gated on CD45$^+$ in SP (B) and BM (C) is shown. The mean value of the absolute number of human CD19$^+$ cells in the BM is shown (D). The mean value of the absolute number of human CD19$^+$ cells and of AnnV$^-$PI$^+$ cells gated on hCD19$^+$ cells in SP is shown (E).

Data are from one representative experiment of three. Statistical analysis: *p < 0.05 and **p < 0.01, Student's t test.

(F–I) i.v. MEC1 challenged (day 0) Rag2$^{-/-}\gamma c^{-/-}$ mice were treated i.v. (days +11 and +25) with 30 mg/kg anti-CSF1R mAb (n = 7, white circles) or left untreated (n = 7, black circles) and killed at days 27 and 29, 48 hr and 96 hr after the last mAb injection (F). The mean value of the absolute number of human CD19$^+$ cells and of AnnV$^-$PI$^+$ cells gated on hCD19$^+$ cells in SP at days 27 and 29 is shown (G). The mean value of the absolute number of CD11b$^+$ F4/80$^+$ cells gated on CD45$^+$ in SP at day 27 is shown (H). The mean value of the absolute number of CD11b$^+$ MRC1$^+$ cells to the CSF1R$^+$ macrophage pool gated on CD45$^+$ in SP at day 27 is shown (I).

Data are from one representative experiment of two. Statistical analysis: *p < 0.05, Student's t test.

See also Figure S4.

already seen in CLL patients with agents targeting BCR signaling (e.g., ibrutinib), which does not indicate disease progression (Byrd et al., 2013). As mAb treatment increased the percentage of CD19$^+$CD20$^+$ circulating leukemic cells (Figure 5C), we tested a two-pronged approach by combining the anti-CSF1R mAb with the glycoengineered type II CD20 mAb, GA101 (Mössner et al., 2010) (Figure 5D). Of note, anti-mouse CSF1R mAb favorably impacted on the survival of mice as single agent (p = 0.0056, αCSF1R mAb versus untreated) and even more significantly in combination settings (p = 0.0082, αCD20 → αCSF1R mAb versus αCD20 mAb; p = 0.01, αCSF1R → αCD20 mAbs versus αCD20 mAb) (Figure 5E).

Considering the reduced CD20 expression on CLL cells and their impaired susceptibility to anti-CD20 mAbs observed in ongoing clinical studies combining anti-CD20 mAbs and promising new drugs such as ibrutinib (Skarzynski et al., 2015), the additive therapeutic effect of CSF1R inhibition and anti-CD20 mAb we here describe pave the way toward important therapeutic strategies for CLL and B lymphoid malignancies.

Leukemic Cell Death Induced by Macrophage Targeting Is TNF Dependent

As a next step we evaluated how leukemic cells were affected by macrophage targeting. Clodrolip and anti-human CSF1R mAb have no direct toxicity on leukemic B cells in vitro, as shown by cytotoxicity assays performed on MEC1 cells (Figure S5A). We therefore investigated alternative mechanisms whereby clodrolip and anti-CSF1R may induce leukemic cell death in vivo. To address this question, Rag2$^{-/-}\gamma c^{-/-}$ mice transplanted i.v. with MEC1 cells were macrophage-depleted by i.v. clodrolip injection every 3 days starting at day −1 (7 consecutive injections) and sacrificed 1 day after the last treatment (Figure 6A). The reduction of the leukemic (Figure 6B) and monocyte/macrophage (Figures 6C–6E) cell burden induced by clodrolip paralleled the induction of apoptosis of leukemic cells in all tissues, as shown by the significantly increased frequency of CD19$^+$ AnnV$^+$PI$^+$ late-apoptotic cells in the SP and BM and of CD19$^+$ AnnV$^-$PI$^+$ necrotic cells in the PB (Figures 6F and 6G). These results confirmed the increase of CD19$^+$ AnnV$^-$PI$^+$ necrotic cells already observed in the SP of anti-CSF1R mAb-treated mice (Figure 4G). The interaction between leukemic B cells and monocytes/macrophages (Movies S1 and S2) and the induction of leukemic B cells apoptosis upon clodrolip (Movie S3) were also visualized in a time-course experiment whereby GFP-labeled monocytes/macrophages were added to leukemic cells from *Eμ-TCL1* transgenic mice in the absence or presence of clodrolip. Interestingly, annexin

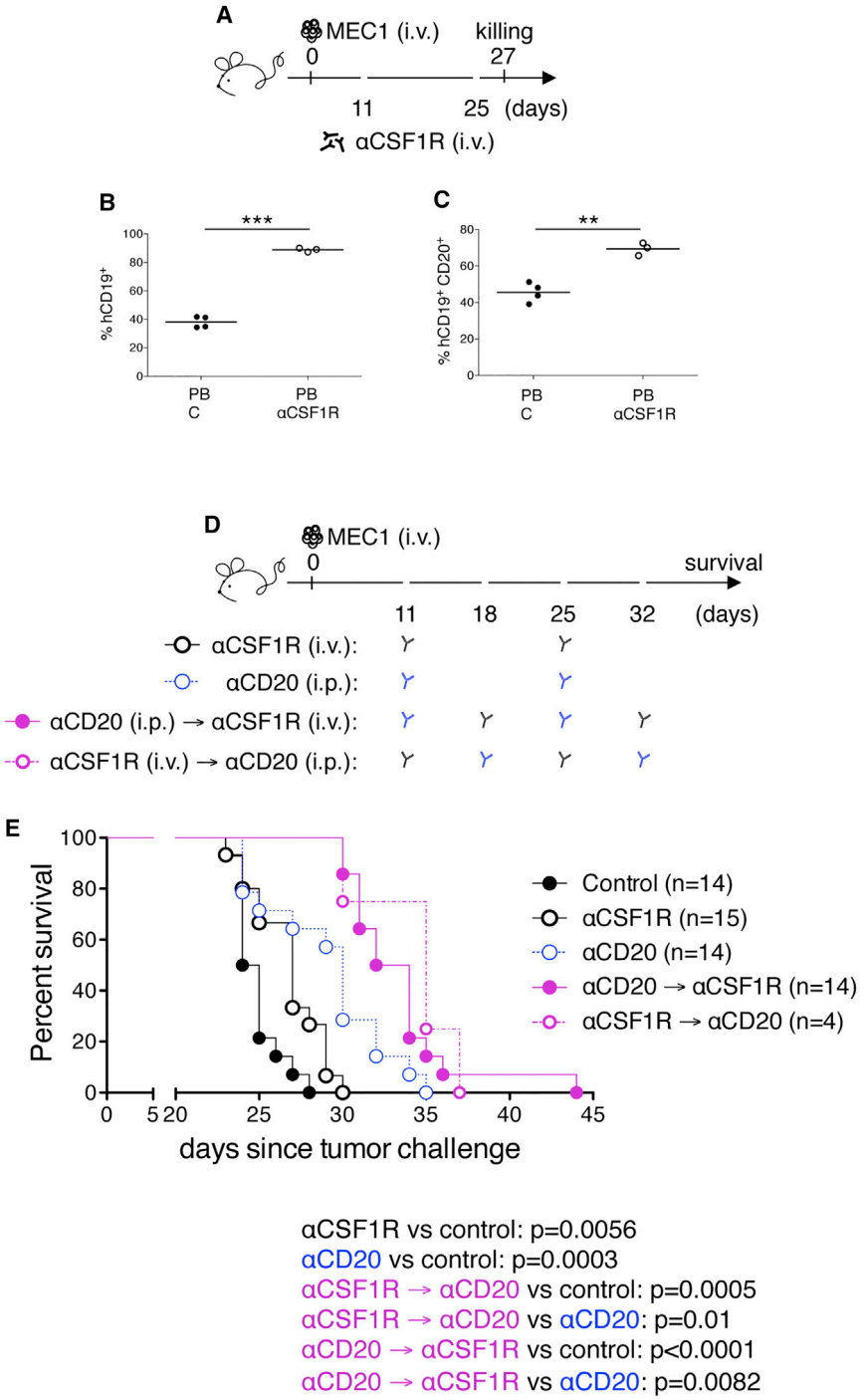

Figure 5. Anti-leukemic Effect and Survival Impact of Anti-CSF1R mAb in the CLL Xeno-transplantation System

(A–C) i.v. MEC1 challenged (day 0) Rag2$^{-/-}\gamma c^{-/-}$ mice were treated i.v. (days +11 and +25) with 30 mg/kg anti-CSF1R mAb (n = 3, white circles) or left untreated (n = 4, black circles) and killed at day 27 (A). The mean value of the percentage of hCD19$^+$ (B) and of hCD19$^+$ CD20$^+$ (C) cells in PB is shown in graphs.

Data are from one representative experiment of two. Statistically significant differences were calculated using the Student's t test (**$p < 0.01$ and ***$p < 0.001$).

(D and E) i.v. MEC1 challenged (day 0) Rag2$^{-/-}\gamma c^{-/-}$ mice were left untreated (n = 14, black circles) or treated with 30 mg/Kg i.v. anti-CSF1R mAb (n = 15, white circles; days +11 and +25) or 30 mg/kg i.p. anti-CD20 mAb GA101 (n = 14, blue circles; days +11 and +25) or 30 mg/kg i.p. anti-CD20 mAb GA101 (day +11, +25) + 30 mg/kg i.v. anti-CSF1R mAb (days +18 and +32) (n = 14, full violet circles) or 30 mg/kg i.v. anti-CSF1R mAb (days +11 and +25) + 30 mg/kg i.p. anti-CD20 mAb GA101 (days +18 and +32) (n = 4, empty violet circles) and monitored for survival (D). The Kaplan-Meier survival curve is shown (E), and statistical analysis was performed using the log-rank test. αCSF1R versus control: p = 0.0056; αCD20 versus control: p = 0.0003; αCD20 → αCSF1R versus control: $p < 0.0001$; αCD20 → αCSF1R versus αCD20: p = 0.0082; αCSF1R → αCD20 versus control: p = 0.0005; αCSF1R → αCD20 versus αCD20: p = 0.01.

V/propidium iodide (AnnV/PI) staining and flow cytometry analysis showed that the induction of leukemic cell apoptosis by clodrolip occurred only in the presence of monocytes and macrophages (Figure S5B).

To investigate the cell death pathways induced in leukemic cells via clodrolip-mediated macrophage killing, we purified CD19$^+$ MEC1 cells from the BM of transplanted Rag2$^{-/-}\gamma_c^{-/-}$ mice and evaluated, at the RNA level by qPCR, the expression of key effector molecules involved in TNF-, TRAIL-, reactive oxygen species (ROS)-, and FAS/FASL-regulated cell death pathways. As for the TNF pathway, we observed upregulated expression of *TNFR1*, *FADD*, *BID*, *BAX*, and *CASP3* (Figure S5C). Interestingly we also found upregulated levels of *TRAIL-R2* and *AIFM1* (Figure S5C), the latter being involved in ROS-mediated dell death (Joza et al., 2009).

To confirm the involvement of TNF (Figure S5C) in the mechanism of leukemia cell death induced by macrophage targeting, we utilized etanercept, a soluble TNF receptor fusion protein (Deeg et al., 2002), in xeno-transplanted Rag2$^{-/-}\gamma_c^{-/-}$ mice treated either with clodrolip or CSF1R mAb. Rag2$^{-/-}\gamma_c^{-/-}$ mice transplanted i.v. with MEC1 cells and injected with clodrolip (i.v., days +11 and +25) and with etanercept (i.p., starting at day +10) were sacrificed 24 hr after the last clodrolip injection (Figure 6H). Etanercept partially rescued clodrolip-induced leukemic cell depletion in the BM (Figure 6I).

In xeno-transplanted mice treated i.v. with the CSF1R mAb (days +11 and +25) and sacrificed 96 hr after the last injection

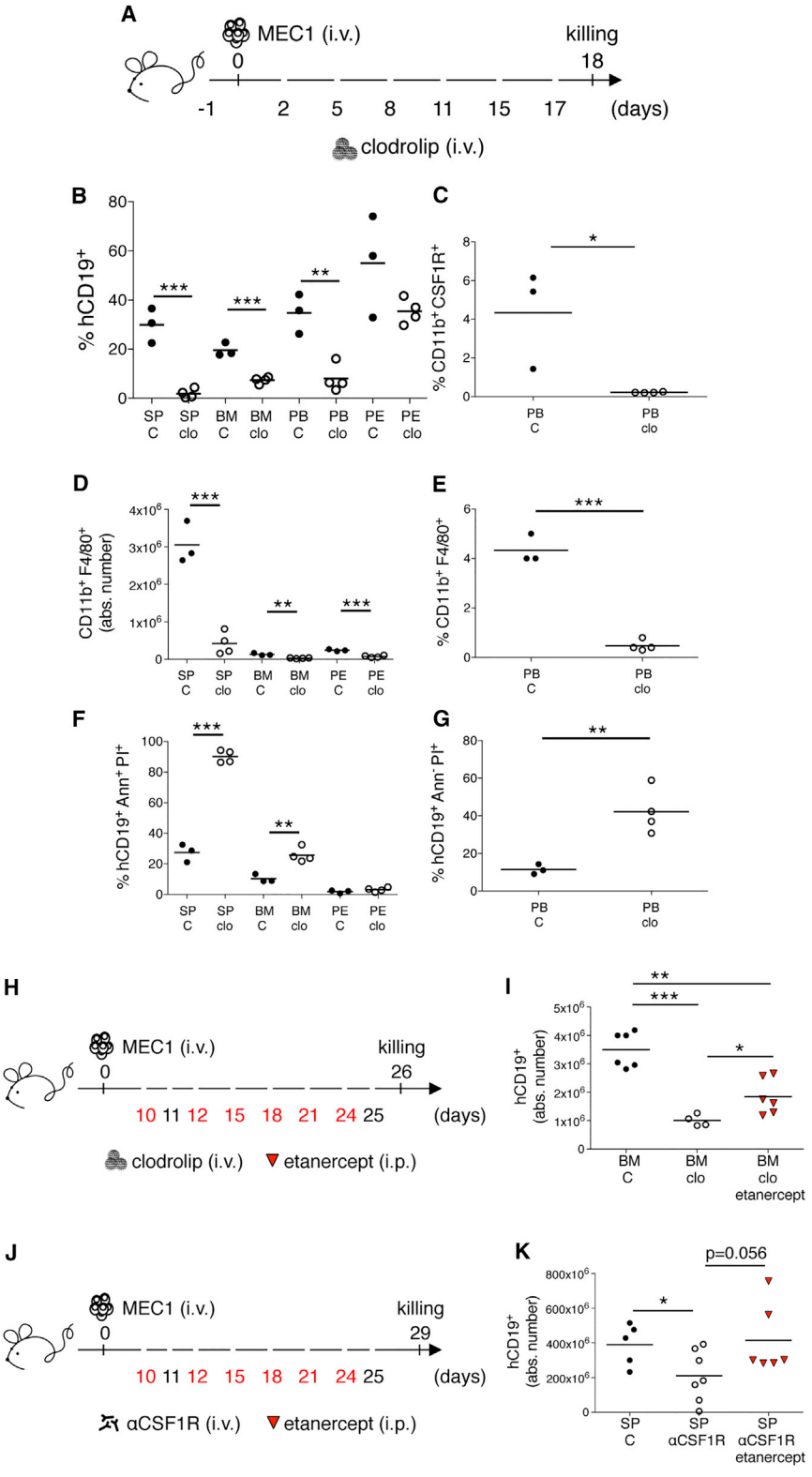

Figure 6. TNF-Dependent Macrophage-Mediated Mechanism of In Vivo Leukemic Cell Death

(A–G) i.v. MEC1 challenged (day 0) Rag2$^{-/-}\gamma c^{-/-}$ mice were either pretreated starting from day −1 every 3 days with 200 μl i.v. clodrolip (n = 4, white circles) or left untreated (n = 3, black circles) and were analyzed by flow cytometry (A). The mean value of the percentage of human CD19$^+$ cells in SP, BM, PB, and PE is shown (B). The mean value of the relative contribution of CD11b$^+$ CSF1R$^+$ cells gated on CD45 in PB is shown (C). The mean value of the absolute number or of the percentage of CD11b$^+$ F4/80$^+$ cells gated on CD45 in SP, BM, PE (D), and PB (E) is shown. The mean value of the relative contribution of AnnV$^+$ PI$^+$ cells gated on hCD19$^+$ cells in SP, BM, and PE (F) and of the relative contribution of AnnV$^-$ PI$^+$ cells gated on hCD19$^+$ cells in PB (G) is shown. Statistical significance was analyzed by Student's t test (*p < 0.05, **p < 0.01, and ***p < 0.001).

(H and I) i.v. MEC1 challenged (day 0) Rag2$^{-/-}\gamma c^{-/-}$ mice were left untreated (n = 6, black circles) or treated i.v. (days +11 and +25) with 60 μl clodrolip (n = 4, white circles) or with 60 μl clodrolip (days +11 and +25) + 10 mg/kg etanercept (i.p., days +10, +12, +15, +18, +21, and +24) (n = 6, red triangles) and killed at day 26 (H). The mean value of the absolute number of human CD19$^+$ cells in the BM is shown (I). Statistical significance was analyzed by Student's t test (*p < 0.05, **p < 0.01, and ***p < 0.001).

(J and K) i.v. MEC1-challenged (day 0) Rag2$^{-/-}\gamma c^{-/-}$ mice were left untreated (n = 5, black circles) or treated i.v. (days +11 and +25) with 30 mg/kg anti-CSF1R mAb (n = 7, white circles) or with 30 mg/kg anti-CSF1R mAb (days +11 and +25) + 10 mg/kg etanercept (i.p., days +10, +12, +15, +18, +21, and +24) (n = 6, red triangles) and killed at day 29 (J). The mean value of the absolute number of human CD19$^+$ cells in the SP is shown in graph (K). Statistical significance was analyzed by Student's t test. *p < 0.05.

See also Figure S5 and Movies S1, S2, and S3.

of the mAb (Figure 6J), the anti-leukemic effect was abrogated in the SP when TNF pathway was blocked in vivo by etanercept (Figure 6K).

Furthermore, we functionally inactivated the FAS/FASL signaling by using the blocking antibody clone Kay-10 (BioLegend) in the *Eμ-TCL1* tg transplantation system. FASL blocking did not abrogate the leukemic cell depletion of transplanted mice treated with clodrolip (Figures S5D–S5G) or with aCSF1R (Figures S5H–S5J). The same clodrolip results were confirmed by transplanting leukemic B cells into *Fasl*^{gld} mice, carrying a null-function mutation of the *Fasl* gene (Figures S5E–S5G).

These findings let us conclude that macrophage killing sensitizes leukemic cells to apoptosis mainly via induction of TNF signaling.

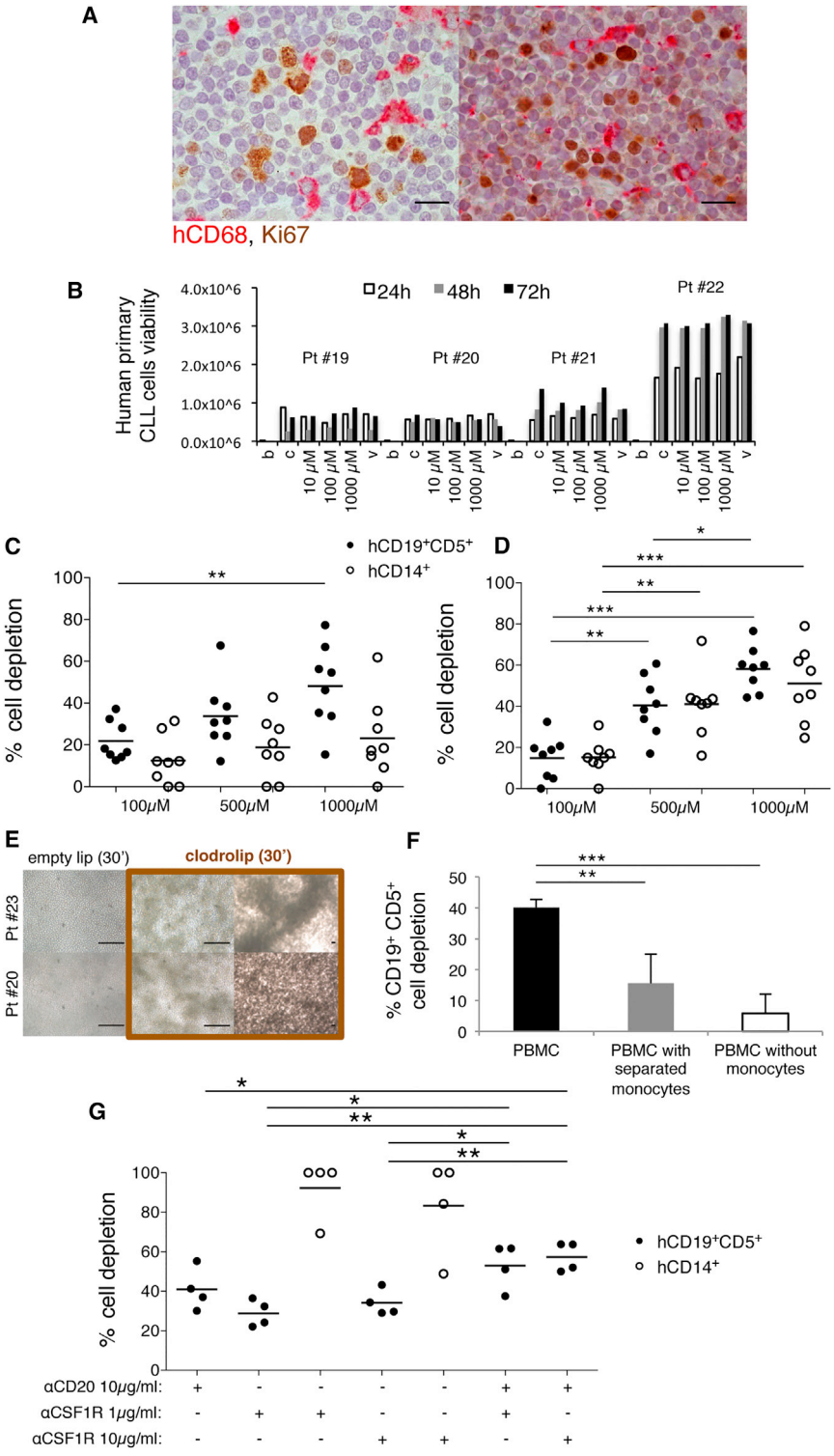

Figure 7. Monocytes/Macrophages and Leukemic Cells in Humans

(A) Immunohistochemistry stain for human CD68 and Ki67 in two representative lymph node sections from CLL patients. Scale bars, 20 μm.

(B) Human primary CLL cells obtained from CLL patients (n = 4, patients #19–22) were plated in 96-well plates alone (c), with increasing concentrations of clodrolip (10 μM, 100 μM, and 1,000 μM) or with PBS liposomes (v, 1,000 μM) and a luminescent assay was performed 24, 48, and 72 hr later to evaluate primary CLL cell sensitivity to the drug (b, background).

(C and D) hCD19$^+$ CD5$^+$ (black circles) and hCD14$^+$ (white circles) depletion after 30 min (C, n = 8) and 24 hr treatment (D), n = 8) with 100 μM, 500 μM, or 1,000 μM clodrolip was calculated by the following formula: 100 - % remaining cells, where % remaining cells = (Absolute number in treated samples/Absolute number in untreated samples) × 100. Horizontal bars represent the mean value (*$p < 0.05$, **$p < 0.01$, and ***$p < 0.001$, Student's t test).

(E) Unseparated PBMCs from CLL patients #20 and #23 in 12-well plates after 30-min treatment with 1,000 μM clodrolip or empty liposomes were photographed with Nikon microscope. Scale bars, 100 μm.

(F) Human primary CD14$^+$ cells obtained from CLL patients (n = 4) were separated from total PBMCs, seeded or not on a transwell chamber (0.4 μm pore size) with 1,000 μM clodrolip or PBS liposomes, while the remaining CD14$^-$ PBMCs or total PBMCs were seeded in the lower part of the chamber. CD19$^+$ CD5$^+$ cell depletion (mean ± SD) of unseparated PBMCs (black bar), PBMCs with separated monocytes (gray bar), and PBMCs without monocytes (white bar) after 24 hr treatment was calculated by the following formula: 100 − % remaining cells, where % remaining cells = (Absolute number in treated samples/Absolute number in untreated samples) × 100. **$p < 0.01$ and ***$p < 0.001$, Student's t test

(G) hCD19$^+$ CD5$^+$ (black circles) and hCD14$^+$ (white circles) depletion after 48 hr (n = 4) with anti-CD20 mAb GA101 10 μg/ml, anti-human CSF1R mAb RG7155 (1–10 μg/ml), anti-CD20 mAb GA101 10 μg/ml + anti-human CSF1R mAb RG7155 (1–10 μg/ml) was calculated by the following formula: 100 − % remaining cells, where % remaining cells = (Absolute number in treated samples/Absolute number in untreated samples) × 100. Horizontal bars represent the mean value (*$p < 0.05$ and **$p < 0.01$, Student's t test).

See also Figure S6.

Targeting Human Primary CLL Cells by Monocyte/Macrophage Killing

Finally, we applied the relevant molecular and functional information gathered in mouse models to human samples. We first analyzed by immunohistochemistry LN sections from CLL patients and observed the proximity of CD68$^+$ macrophages to proliferating (Ki67$^+$) CLL cells in the proliferation centers (Figure 7A). As a next step, we evaluated whether human primary leukemic cells could be affected by clodrolip. Clodrolip had no direct toxic effect in vitro on leukemic B cells, as shown by cytotoxicity studies performed on MEC1 cells

(Figure S5A) as well as on purified human primary CLL cells (Figure 7B). However, when unfractionated peripheral blood mononuclear cells (PBMCs) of CLL patients (which contained both leukemic and normal hematopoietic cells) were treated with different doses of clodrolip, we observed a marked depletion of both $CD14^+$ monocytes and leukemic B cells, as early as 30 min after treatment (Figure 7C) and even more markedly after 24 hr (Figure 7D). The massive leukemic cell death induced by monocyte killing is shown in Figure 7E. Transwell experiments, performed by seeding PBMCs from CLL patients depleted of monocytes, showed that CLL death is partially dependent on cell-cell contacts (Figure 7F).

We then evaluated the expression of key effector molecules involved in cell death mechanisms in human primary leukemic cells. To this aim, we purified by magnetic negative selection leukemic cells from PBMCs of 24-hr-clodrolip cultures and untreated control cultures. We observed a significant upregulation of *FAS* in all the treated samples analyzed (Figure S6A, n = 3). Besides *FAS*, we observed the upregulation of *TNFR1*, *FADD*, *BID*, and *TRAIL-R2* in one patient's sample (Figure S6B), suggesting that several pathways of cell death (e.g., FAS/FASL, TRAIL, and TNF) may be involved also in human primary CLL cell killing induced by monocytes/macrophages.

To investigate the involvement of TNF and TRAIL in the mechanism of leukemia cell death, we utilized etanercept and a blocking anti-human TRAIL-R2 mAb (Germano et al., 2013). As shown in Figures S6C and S6D, in three out of four samples, the leukemic cell depletion induced by clodrolip was reduced when TNF (Figure S6C) and TRAIL signaling (Figure S6D) were blocked. To conclusively test the efficacy of a macrophage targeting strategy on primary cells from CLL patients, PBMCs were treated with anti-human CSF1R mAb (Figure 7G). We observed a relevant depletion of both $CD14^+$ monocytes and leukemic B cells after 48 hr. More strikingly, the leukemic cell depletion increased significantly when the anti-human CSF1R mAb was associated to GA101 (Figure 7G).

Together, these findings indicate that macrophage killing either restores CLL sensitivity to apoptosis or directly induces their death. They further support the rationale translating these findings into combination therapies.

DISCUSSION

All relevant events in CLL occur in permissive tissue microenvironments where different cell types influence the disease natural history, account for its clinical heterogeneity, and provide the basis for identifying novel treatment targets. We unambiguously demonstrate, at the molecular and functional level, that malignant lymphocytes critically depend on the support of TAMs and provide the proof of principle that the manipulation of leukemic cell/TAM interactions may help designing therapeutic strategies for CLL.

Whole-genome transcriptional analysis indicates that BM monocytes/macrophages exposed to leukemic cells in vivo are enriched for specific genes involved in monocyte/macrophage-B cell interaction, inflammation, and transcription function. Likewise, the leukemic cell transcriptome is modified upon interaction with the BM microenvironment (Figure S7). The upregulation of *Saa3* on monocytes/macrophages highlights the relevance of an inflammatory microenvironment in leukemia engraftment and progression. SAA3 is known to attract monocytes/macrophages, and it may cooperate with interleukin-10 (IL-10) to promote M2-skewed macrophage accumulation (Hao et al., 2012; Hiratsuka et al., 2008; Mantovani et al., 2004), ultimately attracting leukemic cells. Notably, we found several chemokines (e.g., *CCL2*, *CCL17*, and *CCL22*) upregulated in leukemic MEC1 cells consistent with previous gene expression studies of leukemic cells from CLL patients (Burger et al., 2009; Herishanu et al., 2011). In keeping with its expression in human NLCs (Filip et al., 2013), the upregulation of ICAM1 in human classical monocytes was particularly relevant. Inhibition of ICAM1 in vivo confirmed its role in the interaction of CLL cells with $CD11b^+$ cells. We also observed an upregulation of several known CLL players: *CXCR4* and *CXCR5* (Burger et al., 2000; Bürkle et al., 2007); *NOTCH1* (Puente et al., 2011), which is associated with poor prognosis (Fabbri et al., 2011) and was shown to improve leukemic cell survival and resistance to apoptosis (Arruga et al., 2014); *BIRC3*, a prognostic factor (Cortese et al., 2014) contributing to drug resistance (Rossi et al., 2012); and *PTEN*, involved in molecular pathology (Leupin et al., 2003), which may represent a further prognostic factor (Beldjord et al., 2014). An unexpected finding was the downregulation of *RNASET2* transcript in leukemic cells. We previously demonstrated that in ovarian tumorigenesis RNASET2 oncosuppressive activity is associated with in vivo recruitment of macrophages (Acquati et al., 2011) and that its loss of function induces a microenvironment imbalance toward M2 tumorigenic macrophages, with consistent depletion of anti-tumorigenic M1 macrophages (Acquati et al., 2013). Our present finding suggests the possibility that *RNASET2* may have a similar role also in leukemogenesis. Another intriguing observation is the upregulation of *CEBPB* in CLL cells hinting at a possible role for this transcription factor, as recently described for C/EBPα in acute myeloblastic leukemia (Roe and Vakoc, 2014). Overall, the scenario emerging from mouse findings (Figure S7) emphasizes the BM as a critical niche for the leukemic clone to engraft and progress with the help of monocytes/macrophages. In turn, leukemic infiltration induces changes of myeloid function during leukemia development and progression. Our data on the anti-CSF1R mAb, known to prevent the formation of new macrophages by inducing apoptosis or inhibiting monocyte differentiation, substantiate the dependence of the leukemic clone on monocytes/macrophages especially in the BM niche, where normally CSF1 induces differentiation and maturation of monocytes (MacDonald et al., 2010; Ries et al., 2014).

The proof of principle that monocyte/macrophage depletion results in an anti-leukemic effect was obtained by clodrolip killing. The results obtained with the therapeutically relevant anti-CSF1R mAb paralleled those obtained with clodrolip. In different mouse models macrophage targeting impairs CLL cell engraftment and, even more interestingly associates with a striking anti-leukemic effect and a significant improvement of mouse survival. The depletion of the monocyte/macrophage pool goes along with the apoptosis of leukemic cells. The molecular mechanisms accounting for the leukemic cell death in vivo appear to entail the RNA upregulation of key molecules of the TNF pathway. Macrophage targeting sensitizes leukemic cells

to apoptosis via induction of TNF signaling and triggers their death through a TNF-dependent mechanism.

As for solid tumors (Ries et al., 2014; Ruffell and Coussens, 2015), we found that CSF1R inhibition selectively targets TAMs and alters the microenvironment toward an anti-leukemic phenotype. Furthermore, at variance with clodrolip, the antibody induced lymphocytosis, i.e., increased circulating leukemic cells expressing CD20 molecule, as it has been observed with BCR-targeting drugs (Byrd et al., 2013). This observation suggested a treatment strategy based upon the combination of two different antibodies, one targeting TAMs and the other targeting $CD20^+$ circulating cells. Our in vitro findings on human primary CLL cells and the survival improvement of xeno-transplanted mice upon the combined treatment corroborated the strong potential of this strategy.

The information obtained in mouse models was reproduced in human samples at the preclinical level. The close proximity of $CD68^+$ macrophages to $Ki67^+$ CLL cells in the lymph node proliferation centers suggests that interfering with such interaction might actually provide an amplification of the death signal. As MEC1 cells, purified primary leukemic cells are also unaffected by clodrolip treatment in vitro, which causes a marked depletion of CLL cells only in the presence of $CD14^+$ monocytes, confirming the monocyte/macrophage dependency of human leukemic cells. *FAS*, a member of the TNFR family, was found upregulated in human primary CLL cells exposed to clodrolip, together with other key molecules of the FAS/FASL, TNF, and TRAIL pathways of cell death. Primary CLL cells do not express TNF receptors in vivo (Digel et al., 1990), but cytokines such as IL-2 are known to influence their expression (Digel et al., 1990). It is thus conceivable that in our system macrophages undergoing rapid and massive apoptosis may release cytokines and growth factors capable of upregulating TNF receptors on leukemic cells and of restoring their sensitivity to apoptosis. This possibility is corroborated by our findings upon TNF-blocking via etanercept.

In conclusion, our results indicate that CLL cell growth in vivo is critically dependent on the support of TAMs and show the tangible positive effects of manipulating such support. The possibility of utilizing drugs and monoclonal antibodies currently in early or advanced clinical development may pave the way to novel treatment approaches in CLL. As an example, our results suggest the possibility of extending to CLL the use of the drug trabectedin, which targets and kills macrophages via the TRAIL receptor and has shown promising results in solid tumors (Germano et al., 2013). Furthermore, our findings on CSF1R inhibition indicate that the clinical use of this type of antibody, possibly in combination with anti-CD20 mAb, is more than worth exploring in CLL. Finally, as the relevance of the inflammatory environment is emerging in different B cell tumors (Hope et al., 2014), it can be predicted that targeting the critical role of TAMs will not be restricted to CLL; rather, it will become a strategy generally applicable to chronic B cell malignancies.

EXPERIMENTAL PROCEDURES

Mice

All mice were housed and bred in a specific pathogen-free animal facility, treated in accordance with the European Union guidelines and with the approval of the San Raffaele Scientific Institute Institutional Ethical Committee. $Rag2^{-/-}\gamma c^{-/-}$ mice on BALB/c background were kindly provided by CIEA and Taconic, *Eμ-TCL1* transgenic mice on a C57BL/6 background were kindly provided by Dr. Byrd, and wild-type C57BL/6 mice were supplied by Charles River Laboratories. Macrophage fas-induced apoptosis (MAFIA) transgenic mice, expressing a bicistronic mRNA encoding both EGFP and transgenic cytoplasmic FAS domains under the control of the c-fms promoter (Burnett et al., 2004), were purchased from Jackson Laboratory. B6Smn.C3-*Fasl*^{gld}/J mice carrying a null-function mutation of the *Fasl* gene were purchased from Jackson Laboratory.

Cells and Reagents

Human primary samples were obtained from RAI stage 0-1 CLL patients, after informed consent as approved by the Institutional Ethical Committee (protocol VIVI-CLL) of San Raffaele Scientific Institute (Milan, Italy) in accordance with the Declaration of Helsinki.

The MEC1 CLL cell line was obtained from Deutsche Sammlung von Mikroorganismen und Zellkulturen (DSMZ) and cultured in RPMI 1640 medium (Invitrogen) with 10% fetal bovine serum and gentamicin (15 μg/ml; Sigma-Aldrich). Clodrolip and phosphate buffer solution liposomes were purchased from ClodLip B.V. Anti-mouse CSF1R antibody 2G2 and anti-human CSF1R antibody emactuzumab (RG7155) (Ries et al., 2014) were provided by Roche Innovation Center Penzberg, Germany. Anti-human CD20 GA101 (Mössner et al., 2010) was provided by Roche Innovation Center Zurich, Switzerland.

In Vivo Studies

For xenograft studies, 8-week-old $Rag2^{-/-}\gamma c^{-/-}$ mice were challenged either i.v. or s.c. with 10×10^6 MEC1 cells in 0.1 ml saline through a 27G needle. Depending on the experiments mice were injected with clodrolip, anti-mouse CSF1R mAb, or anti-human CD20 GA101 mAb. For transgenic transplantation studies, C57BL/6 male mice were challenged i.p. (day 0) with 10×10^6 cells purified from the spleen of leukemic male *Eμ-TCL1* transgenic mice. Depending on the experiments, mice were treated with clodrolip or anti-CSF1R mAb at different doses and schedules. For detailed doses/schedules and functional studies with etanercept and blocking mAbs, see Supplemental Experimental Procedures.

Murine Cell Preparations

PB, PE, SP, and femurs were collected from mice and cells were isolated. Erythrocytes from BM, PE, SP, and PB samples were lysed by incubation for 5 min at room temperature in ammonium chloride solution (ACK) lysis buffer (0.15 M NH_4Cl, 10 mM $KHCO_3$, and 0.1 mM Na_2EDTA [pH 7.2–7.4]). After blocking fragment crystallizable (Fc) receptors with Fc block (BD Biosciences) for 10 min at room temperature, cells from PB, BM, PE, and SP were stained with the antibodies (15 min at 4°C) listed in Supplemental Experimental Procedures and analyzed with a Beckman Coulter FC500 flow cytometer. Absolute numbers were obtained by multiplying the percentage of the cells by the total number of splenocytes, peritoneal cells, or BM cells flushed from one femur (except for Figures 1B–1E, where the absolute number refers to the total BM cells flushed from both femurs and tibias).

In Vitro Cultures and Cell-Depletion Assays from CLL Samples

Fresh PBMCs from untreated CLL patients were seeded, as triplicates, at 3×10^6 cells/ml in culture medium and treated with clodrolip or PBS liposomes (100, 500, or 1,000 μM) for 30 min and 24 hr in the presence or absence of etanercept (10 μg/ml), a TNF-α antagonist from Pfizer, or anti-TRAIL-R2 (human, 1 μg/ml) mAb (HS201) from Adipogen AG. For CSF1R inhibition studies, PBMCs from CLL patients were treated 48 hr with anti-human CSF1R mAb (1–10 μg/ml) or with anti-human CSF1R mAb + anti-CD20 mAb GA101 (10 μg/ml). The specific percentage of remaining leukemic $CD19^+CD5^+$ or $CD14^+$ cells in treated samples was calculated as (absolute number in treated samples/absolute number in control samples) × 100. For each condition, the absolute number of remaining cells was calculated as total viable cell number (trypan blue exclusion determination) × % of viable cells (flow cytometry determination). Then, specific cell depletion was calculated as follow: 100 − % specific remaining cells, as described previously (Laprevotte et al., 2013).

Histopathology and Immunohistochemistry

Tissues were fixed in 4% formalin for 12 hr, then embedded and included in paraffin wax. Sections (5 mm thick) were cut and stained with H&E according

Please cite this article in press as: Galletti et al., Targeting Macrophages Sensitizes Chronic Lymphocytic Leukemia to Apoptosis and Inhibits Disease Progression, Cell Reports (2016), http://dx.doi.org/10.1016/j.celrep.2016.01.042

to standard protocols. Microscopic specimens were evaluated by a pathologist in a blinded fashion. For immunohistochemistry, see Supplemental Experimental Procedures.

Gene Expression Profiling Analysis

BM microenvironment cells were flushed from mice femurs and separated from leukemic MEC1 cells, which were positively selected by human anti-CD19 beads and blocked on Miltenyi MS columns. hCD19^{-} cells were secondary enriched of monocytes/macrophages by depletion of T, natural killer, dendritic cells, progenitors, granulocytes, and red blood cells with an EasySep negative selection monocyte enrichment kit on an EasySep Magnet (STEMCELL Technologies), following the manufacturer's indications. RNA extraction was performed using RNeasy Mini Kit (QIAGEN). 200 ng total RNA samples was processed using an Illumina TotalPrep Amplification kit (Ambion Life Technologies), strictly adhering to the manufacturer's protocol. Subsequently, biotin-labeled cRNA was hybridized on a MouseWG-6 v2.0 Expression BeadChip (harboring probes for ~45,000 transcript) or HumanHT-12 v4 BeadChip (harboring probes for ~47,000 transcript) (Illumina) for 16 hr, followed by Cy3 staining. Following hybridization, the BeadChip underwent a washing and streptavidin-Cy3 (GE Healthcare Bio-Sciences) conjugate staining protocol. Once the BeadChip was processed it was scanned with an Illumina BeadArray Reader. In brief, arrays were scanned on a BeadScan instrument, and fluorescence intensities were extracted and summarized using the BeadStudio software (Illumina), resulting in a set of summarized fluorescence measurements. For detailed microarray analysis, see Supplemental Experimental Procedures.

Statistical Analysis

Statistical analyses were performed with the use of the Student's t test. Data are expressed as mean ± SD, and comparison of growth curves was considered statistically significant for $p < 0.05$. Comparison of survival curves was performed with the use of the log-rank test. For microarray analysis, see Supplemental Experimental Procedures.

ACCESSION NUMBERS

The accession numbers for the GEP human and mouse studies are GEO: GSE57787 and GSE57785, respectively.

SUPPLEMENTAL INFORMATION

Supplemental Information includes Supplemental Experimental Procedures, seven figures, one table, and three movies and can be found with this article online at http://dx.doi.org/10.1016/j.celrep.2016.01.042.

AUTHOR CONTRIBUTIONS

G.G. designed and performed experiments, analyzed the data, and wrote the paper; C.S. performed in vitro and molecular studies and assisted in writing the paper; F.B. and P.R. performed in vitro studies; T.V.R. performed in vivo and molecular studies; M.R., D.L., and D.C. assisted in designing GEP studies and performed GEP statistical analysis; G.S. performed in vivo experiments and assisted in analyzing data; L.S. assisted in human studies; M.P. analyzed data, interpreted histology, and reviewed the paper; M.R. performed histology; A.C. assisted in designing cell death studies; A.A. assisted in flow cytometry studies; N.v.R. provided clodrolip; C.K. provided mAb and assisted in anti-CD20 studies; C.H.R. provided mAb, assisted in anti-CSF1R inhibition studies, and reviewed the paper; P.G. reviewed the paper; M.D.P. co-supervised the project, interpreted the results, and wrote the paper; F.C.-C. guided research, analyzed data, and wrote the paper; and M.T.S.B. designed and supervised the project, performed experiments, analyzed the data, and wrote the paper.

CONFLICTS OF INTEREST

C.H.R. and C.K. are employees of Roche. This study was supported by Roche (M.T.S.B. and P.G).

ACKNOWLEDGMENTS

Eμ-TCL1 transgenic mice were a kind gift of J. Byrd and C.M. Croce (Columbus, OH). Rag2$^{-/-}\gamma c^{-/-}$ mice on BALB/c background were kindly provided by CIEA and Taconic. We thank G. Tonon for helpful suggestions and discussion. We thank F. Curnis for providing etanercept. This study was supported by Program Molecular Clinical Oncology-5 per mille number 9965 (to F.C.-C., P.G., A.C., and M.D.P.), Associazione Italiana per la Ricerca sul Cancro AIRC (Italy), Ricerca Finalizzata (Ministero della Salute, Italy), and Roche (to M.T.S.B. and P.G.). C.H.R. and C.K. are employees of Roche; all the remaining authors declare no competing financial interests. Figures were produced using Servier Medical Art (http://www.servier.com).

Received: September 5, 2014
Revised: December 8, 2015
Accepted: January 9, 2016
Published: February 11, 2016

REFERENCES

Acquati, F., Bertilaccio, S., Grimaldi, A., Monti, L., Cinquetti, R., Bonetti, P., Lualdi, M., Vidalino, L., Fabbri, M., Sacco, M.G., et al. (2011). Microenvironmental control of malignancy exerted by RNASET2, a widely conserved extracellular RNase. Proc. Natl. Acad. Sci. USA *108*, 1104–1109.

Acquati, F., Lualdi, M., Bertilaccio, S., Monti, L., Turconi, G., Fabbri, M., Grimaldi, A., Anselmo, A., Inforzato, A., Collotta, A., et al. (2013). Loss of function of Ribonuclease T2, an ancient and phylogenetically conserved RNase, plays a crucial role in ovarian tumorigenesis. Proc. Natl. Acad. Sci. USA *110*, 8140–8145.

Arruga, F., Gizdic, B., Serra, S., Vaisitti, T., Ciardullo, C., Coscia, M., Laurenti, L., D'Arena, G., Jaksic, O., Inghirami, G., et al. (2014). Functional impact of NOTCH1 mutations in chronic lymphocytic leukemia. Leukemia *28*, 1060–1070.

Batista, F.D., and Harwood, N.E. (2009). The who, how and where of antigen presentation to B cells. Nat. Rev. Immunol. *9*, 15–27.

Beldjord, K., Chevret, S., Asnafi, V., Huguet, F., Boulland, M.L., Leguay, T., Thomas, X., Cayuela, J.M., Grardel, N., Chalandon, Y., et al.; Group for Research on Adult Acute Lymphoblastic Leukemia (GRAALL) (2014). Oncogenetics and minimal residual disease are independent outcome predictors in adult patients with acute lymphoblastic leukemia. Blood *123*, 3739–3749.

Bertilaccio, M.T., Scielzo, C., Simonetti, G., Ponzoni, M., Apollonio, B., Fazi, C., Scarfò, L., Rocchi, M., Muzio, M., Caligaris-Cappio, F., and Ghia, P. (2010). A novel Rag2-/-gammac-/–xenograft model of human CLL. Blood *115*, 1605–1609.

Bichi, R., Shinton, S.A., Martin, E.S., Koval, A., Calin, G.A., Cesari, R., Russo, G., Hardy, R.R., and Croce, C.M. (2002). Human chronic lymphocytic leukemia modeled in mouse by targeted TCL1 expression. Proc. Natl. Acad. Sci. USA *99*, 6955–6960.

Burger, J.A., and Gribben, J.G. (2014). The microenvironment in chronic lymphocytic leukemia (CLL) and other B cell malignancies: insight into disease biology and new targeted therapies. Semin. Cancer Biol. *24*, 71–81.

Burger, J.A., Tsukada, N., Burger, M., Zvaifler, N.J., Dell'Aquila, M., and Kipps, T.J. (2000). Blood-derived nurse-like cells protect chronic lymphocytic leukemia B cells from spontaneous apoptosis through stromal cell-derived factor-1. Blood *96*, 2655–2663.

Burger, J.A., Quiroga, M.P., Hartmann, E., Bürkle, A., Wierda, W.G., Keating, M.J., and Rosenwald, A. (2009). High-level expression of the T-cell chemokines CCL3 and CCL4 by chronic lymphocytic leukemia B cells in nurselike cell cocultures and after BCR stimulation. Blood *113*, 3050–3058.

Bürkle, A., Niedermeier, M., Schmitt-Gräff, A., Wierda, W.G., Keating, M.J., and Burger, J.A. (2007). Overexpression of the CXCR5 chemokine receptor, and its ligand, CXCL13 in B-cell chronic lymphocytic leukemia. Blood *110*, 3316–3325.

Burnett, S.H., Kershen, E.J., Zhang, J., Zeng, L., Straley, S.C., Kaplan, A.M., and Cohen, D.A. (2004). Conditional macrophage ablation in transgenic mice expressing a Fas-based suicide gene. J. Leukoc. Biol. *75*, 612–623.

Byrd, J.C., Furman, R.R., Coutre, S.E., Flinn, I.W., Burger, J.A., Blum, K.A., Grant, B., Sharman, J.P., Coleman, M., Wierda, W.G., et al. (2013). Targeting BTK with ibrutinib in relapsed chronic lymphocytic leukemia. N. Engl. J. Med. *369*, 32–42.

Caligaris-Cappio, F., and Ghia, P. (2008). Novel insights in chronic lymphocytic leukemia: are we getting closer to understanding the pathogenesis of the disease? J. Clin. Oncol. *26*, 4497–4503.

Caligaris-Cappio, F., Bertilaccio, M.T., and Scielzo, C. (2014). How the microenvironment wires the natural history of chronic lymphocytic leukemia. Semin. Cancer Biol. *24*, 43–48.

Cortese, D., Sutton, L.A., Cahill, N., Smedby, K.E., Geisler, C., Gunnarsson, R., Juliusson, G., Mansouri, L., and Rosenquist, R. (2014). On the way towards a 'CLL prognostic index': focus on TP53, BIRC3, SF3B1, NOTCH1 and MYD88 in a population-based cohort. Leukemia *28*, 710–713.

De Palma, M., and Lewis, C.E. (2013). Macrophage regulation of tumor responses to anticancer therapies. Cancer Cell *23*, 277–286.

Deeg, H.J., Gotlib, J., Beckham, C., Dugan, K., Holmberg, L., Schubert, M., Appelbaum, F., and Greenberg, P. (2002). Soluble TNF receptor fusion protein (etanercept) for the treatment of myelodysplastic syndrome: a pilot study. Leukemia *16*, 162–164.

Digel, W., Schöniger, W., Stefanic, M., Janssen, H., Buck, C., Schmid, M., Raghavachar, A., and Porzsolt, F. (1990). Receptors for tumor necrosis factor on neoplastic B cells from chronic lymphocytic leukemia are expressed in vitro but not in vivo. Blood *76*, 1607–1613.

Fabbri, G., Rasi, S., Rossi, D., Trifonov, V., Khiabanian, H., Ma, J., Grunn, A., Fangazio, M., Capello, D., Monti, S., et al. (2011). Analysis of the chronic lymphocytic leukemia coding genome: role of NOTCH1 mutational activation. J. Exp. Med. *208*, 1389–1401.

Filip, A.A., Ciseł, B., Koczkodaj, D., Wąsik-Szczepanek, E., Piersiak, T., and Dmoszyńska, A. (2013). Circulating microenvironment of CLL: are nurse-like cells related to tumor-associated macrophages? Blood Cells Mol. Dis. *50*, 263–270.

Germano, G., Frapolli, R., Belgiovine, C., Anselmo, A., Pesce, S., Liguori, M., Erba, E., Uboldi, S., Zucchetti, M., Pasqualini, F., et al. (2013). Role of macrophage targeting in the antitumor activity of trabectedin. Cancer Cell *23*, 249–262.

Hao, N.B., Lü, M.H., Fan, Y.H., Cao, Y.L., Zhang, Z.R., and Yang, S.M. (2012). Macrophages in tumor microenvironments and the progression of tumors. Clin. Dev. Immunol. *2012*, 948098.

Herishanu, Y., Pérez-Galán, P., Liu, D., Biancotto, A., Pittaluga, S., Vire, B., Gibellini, F., Njuguna, N., Lee, E., Stennett, L., et al. (2011). The lymph node microenvironment promotes B-cell receptor signaling, NF-kappaB activation, and tumor proliferation in chronic lymphocytic leukemia. Blood *117*, 563–574.

Herman, S.E., Gordon, A.L., Hertlein, E., Ramanunni, A., Zhang, X., Jaglowski, S., Flynn, J., Jones, J., Blum, K.A., Buggy, J.J., et al. (2011). Bruton tyrosine kinase represents a promising therapeutic target for treatment of chronic lymphocytic leukemia and is effectively targeted by PCI-32765. Blood *117*, 6287–6296.

Hiratsuka, S., Watanabe, A., Sakurai, Y., Akashi-Takamura, S., Ishibashi, S., Miyake, K., Shibuya, M., Akira, S., Aburatani, H., and Maru, Y. (2008). The S100A8-serum amyloid A3-TLR4 paracrine cascade establishes a pre-metastatic phase. Nat. Cell Biol. *10*, 1349–1355.

Hope, C., Ollar, S.J., Heninger, E., Hebron, E., Jensen, J.L., Kim, J., Maroulakou, I., Miyamoto, S., Leith, C., Yang, D.T., et al. (2014). TPL2 kinase regulates the inflammatory milieu of the myeloma niche. Blood *123*, 3305–3315.

Joza, N., Pospisilik, J.A., Hangen, E., Hanada, T., Modjtahedi, N., Penninger, J.M., and Kroemer, G. (2009). AIF: not just an apoptosis-inducing factor. Ann. N Y Acad. Sci. *1171*, 2–11.

Laprevotte, E., Voisin, G., Ysebaert, L., Klein, C., Daugrois, C., Laurent, G., Fournie, J.J., and Quillet-Mary, A. (2013). Recombinant human IL-15 trans-presentation by B leukemic cells from chronic lymphocytic leukemia induces autologous NK cell proliferation leading to improved anti-CD20 immunotherapy. J. Immunol. *191*, 3634–3640.

Leupin, N., Cenni, B., Novak, U., Hügli, B., Graber, H.U., Tobler, A., and Fey, M.F. (2003). Disparate expression of the PTEN gene: a novel finding in B-cell chronic lymphocytic leukaemia (B-CLL). Br. J. Haematol. *121*, 97–100.

Lutzny, G., Kocher, T., Schmidt-Supprian, M., Rudelius, M., Klein-Hitpass, L., Finch, A.J., Dürig, J., Wagner, M., Haferlach, C., Kohlmann, A., et al. (2013). Protein kinase c-β-dependent activation of NF-κB in stromal cells is indispensable for the survival of chronic lymphocytic leukemia B cells in vivo. Cancer Cell *23*, 77–92.

MacDonald, K.P., Palmer, J.S., Cronau, S., Seppanen, E., Olver, S., Raffelt, N.C., Kuns, R., Pettit, A.R., Clouston, A., Wainwright, B., et al. (2010). An antibody against the colony-stimulating factor 1 receptor depletes the resident subset of monocytes and tissue- and tumor-associated macrophages but does not inhibit inflammation. Blood *116*, 3955–3963.

Mantovani, A., Sica, A., Sozzani, S., Allavena, P., Vecchi, A., and Locati, M. (2004). The chemokine system in diverse forms of macrophage activation and polarization. Trends Immunol. *25*, 677–686.

Mössner, E., Brünker, P., Moser, S., Püntener, U., Schmidt, C., Herter, S., Grau, R., Gerdes, C., Nopora, A., van Puijenbroek, E., et al. (2010). Increasing the efficacy of CD20 antibody therapy through the engineering of a new type II anti-CD20 antibody with enhanced direct and immune effector cell-mediated B-cell cytotoxicity. Blood *115*, 4393–4402.

Noy, R., and Pollard, J.W. (2014). Tumor-associated macrophages: from mechanisms to therapy. Immunity *41*, 49–61.

Puente, X.S., Pinyol, M., Quesada, V., Conde, L., Ordóñez, G.R., Villamor, N., Escaramis, G., Jares, P., Beà, S., González-Díaz, M., et al. (2011). Whole-genome sequencing identifies recurrent mutations in chronic lymphocytic leukaemia. Nature *475*, 101–105.

Reinart, N., Nguyen, P.H., Boucas, J., Rosen, N., Kvasnicka, H.M., Heukamp, L., Rudolph, C., Ristovska, V., Velmans, T., Mueller, C., et al. (2013). Delayed development of chronic lymphocytic leukemia in the absence of macrophage migration inhibitory factor. Blood *121*, 812–821.

Ries, C.H., Cannarile, M.A., Hoves, S., Benz, J., Wartha, K., Runza, V., Rey-Giraud, F., Pradel, L.P., Feuerhake, F., Klaman, I., et al. (2014). Targeting tumor-associated macrophages with anti-CSF-1R antibody reveals a strategy for cancer therapy. Cancer Cell *25*, 846–859.

Roe, J.S., and Vakoc, C.R. (2014). C/EBPα: critical at the origin of leukemic transformation. J. Exp. Med. *211*, 1–4.

Rossi, D., Fangazio, M., Rasi, S., Vaisitti, T., Monti, S., Cresta, S., Chiaretti, S., Del Giudice, I., Fabbri, G., Bruscaggin, A., et al. (2012). Disruption of BIRC3 associates with fludarabine chemorefractoriness in TP53 wild-type chronic lymphocytic leukemia. Blood *119*, 2854–2862.

Ruffell, B., and Coussens, L.M. (2015). Macrophages and therapeutic resistance in cancer. Cancer Cell *27*, 462–472.

Skarzynski, M., Niemann, C.U., Lee, Y.S., Martyr, S., Maric, I., Salem, D., Stetler-Stevenson, M., Marti, G.E., Calvo, K.R., Yuan, C., et al. (2015). Interactions between ibrutinib and anti-CD20 antibodies: competing effects on the outcome of combination therapy. Clin Cancer Res. *22*, 86–95.

Sunderkötter, C., Nikolic, T., Dillon, M.J., Van Rooijen, N., Stehling, M., Drevets, D.A., and Leenen, P.J. (2004). Subpopulations of mouse blood monocytes differ in maturation stage and inflammatory response. J. Immunol. *172*, 4410–4417.

Tsukada, N., Burger, J.A., Zvaifler, N.J., and Kipps, T.J. (2002). Distinctive features of "nurselike" cells that differentiate in the context of chronic lymphocytic leukemia. Blood *99*, 1030–1037.

van Rooijen, N., and Hendrikx, E. (2010). Liposomes for specific depletion of macrophages from organs and tissues. Methods Mol. Biol. *605*, 189–203.

Zanesi, N., Aqeilan, R., Drusco, A., Kaou, M., Sevignani, C., Costinean, S., Bortesi, L., La Rocca, G., Koldovsky, P., Volinia, S., et al. (2006). Effect of rapamycin on mouse chronic lymphocytic leukemia and the development of nonhematopoietic malignancies in Emu-TCL1 transgenic mice. Cancer Res. *66*, 915–920.

Zenz, T., Mertens, D., Küppers, R., Döhner, H., and Stilgenbauer, S. (2010). From pathogenesis to treatment of chronic lymphocytic leukaemia. Nat. Rev. Cancer *10*, 37–50.